Computational Design of High-level Interlocking Puzzles

RULIN CHEN, Singapore University of Technology and Design, Singapore
ZIQI WANG, EPFL, Switzerland and ETH Zürich, Switzerland
PENG SONG, Singapore University of Technology and Design, Singapore
BERND BICKEL, IST, Austria

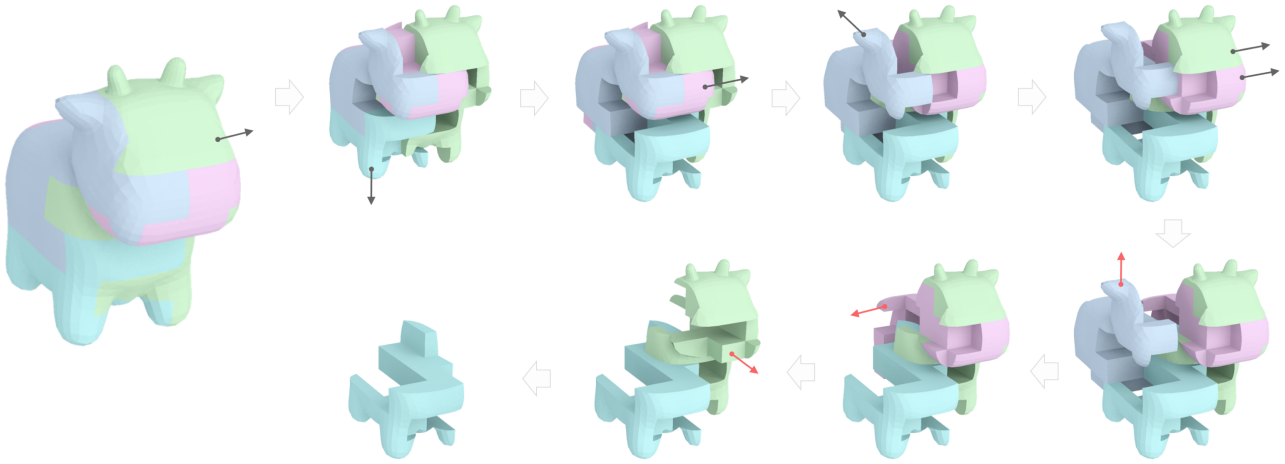

Fig. 1. A 4-piece level-6 interlocking puzzle designed by our approach that requires 6 moves to take out the first piece (in blue color). Each sub-figure shows a configuration of the puzzle pieces in the disassembly plan, where arrows indicate the translational direction to move (in black) or remove (in red) a subassembly to reach the next configuration. Note that the two black arrows in the top right subfigure indicate a single move of a subassembly with two parts.

Interlocking puzzles are intriguing geometric games where the puzzle pieces are held together based on their geometric arrangement, preventing the puzzle from falling apart. *High-level-of-difficulty*, or simply *high-level*, interlocking puzzles are a subclass of interlocking puzzles that require multiple moves to take out the first subassembly from the puzzle. Solving a high-level interlocking puzzle is a challenging task since one has to explore many different configurations of the puzzle pieces until reaching a configuration where the first subassembly can be taken out. Designing a high-level interlocking puzzle with a user-specified level of difficulty is even harder since the puzzle pieces have to be interlocking in all the configurations before the first subassembly is taken out.

In this paper, we present a computational approach to design high-level interlocking puzzles. The core idea is to represent all possible configurations of an interlocking puzzle as well as transitions among these configurations using a rooted, undirected graph called a *disassembly graph* and leverage this graph to find a disassembly plan that requires a minimal number of moves to take out the first subassembly from the puzzle. At the design stage, our algorithm iteratively constructs the geometry of each puzzle piece to expand the disassembly graph incrementally, aiming to achieve a user-specified level of difficulty. We show that our approach allows efficient generation of high-level interlocking puzzles of various shape complexities, including new solutions not attainable by state-of-the-art approaches.

CCS Concepts: • **Computing methodologies** → *Shape modeling*.

Additional Key Words and Phrases: interlocking puzzle, level of difficulty, disassembly planning, computational design

ACM Reference Format:
Rulin Chen, Ziqi Wang, Peng Song, and Bernd Bickel. 2022. Computational Design of High-level Interlocking Puzzles. *ACM Trans. Graph.* 41, 4, Article 150 (July 2022), 15 pages. https://doi.org/10.1145/3528223.3530071

Authors' addresses: Rulin Chen, Singapore University of Technology and Design, Singapore, rulin_chen@mymail.sutd.edu.sg; Ziqi Wang, EPFL, Switzerland and , ETH Zürich, Switzerland, ziqi.wang@inf.ethz.ch; Peng Song, Singapore University of Technology and Design, Singapore, peng_song@sutd.edu.sg; Bernd Bickel, IST, Austria, bernd.bickel@ist.ac.at.

1 INTRODUCTION

Interlocking puzzles are a specific class of 3D geometric puzzles [Cofin 2006], where puzzle pieces interlock with one another, preventing the 3D assembly from falling apart. The aim of the puzzle game is to put together all the puzzle pieces to form a meaningful 3D shape or to disassemble a complete puzzle into individual puzzle pieces. Motivated by their recreational value and geometric beauty, a number of computational approaches have been developed by the graphics community for designing interlocking puzzles [Song et al. 2012; Wang et al. 2018; Xin et al. 2011].

Many existing interlocking puzzles, including those designed by the above computational approaches, can be disassembled by repeating the process of identifying a movable puzzle piece and taking it out directly; see Figure 2 (top) for an example. In other words, these interlocking puzzles assume a monotone and linear disassembly

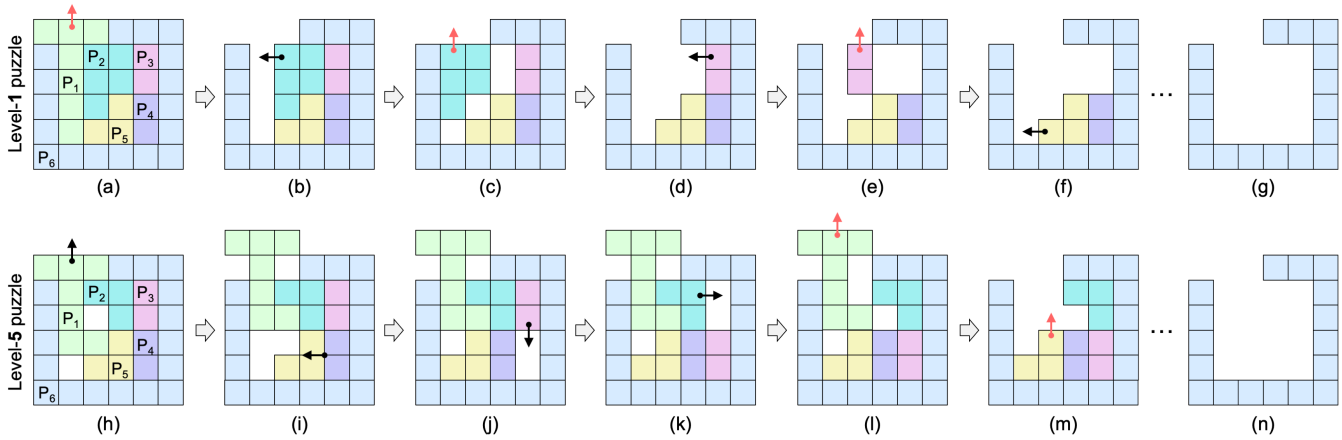

Fig. 2. Comparing a level-1 interlocking puzzle (top) and a level-5 interlocking puzzle (bottom). (Top) The puzzle requires one move to take out the first piece (P_1); each of the remaining puzzle pieces requires two moves to be taken out. (Bottom) The puzzle requires five moves to take out the first piece (P_1), where the 2nd move translates two puzzle pieces (P_4 and P_5) together; after taking out P_1, each of the remaining puzzle pieces can be taken out easily.

plan. In a monotone disassembly plan, there is no need for intermediate placements of puzzle pieces for solving the disassembly problem while in a linear disassembly plan, each disassembly operation involves moving a single puzzle piece relative to the rest of the assembly [Ghandi and Masehian 2015].

To make the disassembly process (i.e., the puzzle game) more intricate and thus more intriguing, we are interested in studying interlocking puzzles that require *non-monotone* and possibly *non-linear* disassembly plans for solving the puzzle in this paper; see Figure 2 (bottom) for an example. To disassemble these puzzles, one needs to try different combinations of moves of the puzzle pieces in order to reach a puzzle configuration (see Figure 2(l)) where the first subassembly can be taken out directly. The *level of difficulty* of these interlocking puzzles are generally assessed by the number of moves required to remove the first subassembly from the puzzle [Coffin 2006]. This is because taking out the first subassembly is the most intriguing part of disassembling interlocking puzzles. Once the first subassembly has been removed, the remaining puzzle can usually be easily disassembled; see Figure 2 (bottom). Puzzles requiring a large number of moves to take out the first subassembly are called *high-level-of-difficulty interlocking puzzles* or simply *high-level interlocking puzzles*.

Solving a high-level interlocking puzzle is a challenging task since one has to find a non-monotone and linear/non-linear plan to disassemble the puzzle, which is known to be an NP-hard problem [Kavraki et al. 1993]. Designing a high-level interlocking puzzle with a user-specified level of difficulty is even more challenging. Besides the difficulty of finding a disassembly plan to ensure that the puzzle has the user-specified level of difficulty, one needs to design the puzzle pieces in a way that they have to be interlocking in all the configurations before the first subassembly is taken out. Due to these challenges, there are not many known high-level interlocking puzzles, and existing ones are mainly limited to holey burr puzzles [Cutler 1988] and cube-shaped puzzles [Gontier 2020].

In this paper, we develop a computational approach for designing new high-level interlocking puzzles according to user specifications, including the puzzle shape, number of puzzle pieces, and level of difficulty. To make the problem tractable, we assume that the puzzle shape is represented as a voxelized model, and disassembly motion is limited to translation along each of the major axes. Our core idea to address the problem is to encode all possible configurations of a given puzzle using a rooted graph data structure, where the level of difficulty corresponds to the length of a shortest path from the root node (i.e., assembled puzzle configuration) to a target node (i.e., configuration where a single subassembly is removed) in the graph. At the design stage, we iteratively construct each puzzle piece to expand the graph data structure incrementally such that potential target nodes can be as far from the root node as possible, aiming to increase the level of difficulty.

Contributions. Specifically, we make the following contributions:

- We propose a graph-based disassembly planner to compute the *exact level of difficulty* of an interlocking puzzle, defined by a *non-monotone* and *linear/non-linear* disassembly plan that requires a minimal number of moves to take out the first subassembly.
- We present a computational framework for constructing the geometry of each voxelized puzzle piece iteratively, guided by the graph-based disassembly planner, to achieve the user-specified level of difficulty.
- We formulate and solve a shape optimization problem to deform an input shape slightly such that we can generate high-level interlocking puzzles with smooth appearance and structurally sound pieces.

Thanks to our shape optimization, our approach is able to design puzzles with both voxelized and smooth appearance. We demonstrate the effectiveness of our computational approach on a variety of shapes, compare it with a state-of-the-art approach [Gontier 2020], and fabricate some of our designed puzzles to validate their level of difficulty; see Figure 1 for an example. Code and data of this paper are at https://github.com/Linsanity81/High-LevelPuzzle.

2 RELATED WORK

Puzzle design. Motivated by recent advances in digital fabrication, the graphics community has raised a great interest in research on computational design for stylized fabrication [Bickel et al. 2018]. Among this line of research, a number of computational methods and tools have been developed for personalized design and fabrication of various kinds of geometric puzzles, including 3D jigsaw puzzles [Elber and Kim 2022], polyomino puzzles [Kita and Miyata 2020; Lo et al. 2009], dissection puzzles [Duncan et al. 2017; Li et al. 2018; Tang et al. 2019; Zhou and Wang 2012], interlocking puzzles [Song et al. 2012; Xin et al. 2011], centrifugal puzzles [Kita and Saito 2020], and twisty puzzles that generalize the Rubik's cube mechanism [Sun and Zheng 2015].

Interlocking assemblies. In an interlocking assembly, there is only one movable part called the *key*, while all other parts, as well as any subset of the parts, are immobilized relative to one another [Song et al. 2012]. A number of computational methods have been developed to construct interlocking assemblies for different applications, including puzzles [Song et al. 2012; Xin et al. 2011], 3D printed objects [Song et al. 2016, 2015; Yao et al. 2017], furniture [Fu et al. 2015; Song et al. 2017], architecture [Wang et al. 2019], and robotic assembly [Zhang and Balkcom 2016; Zhang et al. 2021]. In particular, Wang et al. [2018] developed a unified framework to design interlocking assemblies of different forms by leveraging a graph-based representation.

The main objective of the above works is to make the assembly structurally stable based on interlocking of component parts. Since the parts are preferred to be easily assembled to form the final structure, all these works assume a monotone and linear (dis)assembly plan. Due to this reason, the resulting interlocking assemblies typically have a level 1 difficulty; i.e., the key can be taken out directly with one move. In this paper, we focus on high-level interlocking assemblies. Different from level-1 interlocking assemblies that are interlocking only at the final configuration, high-level interlocking assemblies have to be "interlocking" (i.e., no removable subassembly) in all the configurations before the first subassembly is removed.

High-level interlocking puzzles. Designing high-level interlocking puzzles is much more difficult than designing the above level-1 interlocking assemblies, due to the coupling of two complex subproblems: *disassembly planning* and *geometric design.* The design of a new high-level interlocking puzzle is extremely hard for humans, even for skilled professionals, which perhaps explains why there are not many known high-level interlocking puzzles [Coffin 2006]. Cutler [1988] proposed to use computers to exhaustively try and discover six-piece interlocking holey burr puzzles. He performed a complete analysis of 13,354,991 essentially different puzzle assemblies, among which the highest level found was level-10. Other than exhaustive search, some 3D puzzle designers took a trial-and-error approach by using computer software such as BurrTools by Röver [2013] as a puzzle solver to test if their puzzle designs can be assembled as well as to compute their level of difficulty. Recently, Gontier [2020] developed a genetic algorithm to search for high-level interlocking cubes on supercomputers, and reported four results of interlocking cubes with level 5, 9, 10, and 13, respectively.

The above approaches compute the level of difficulty of a given interlocking puzzle based on a feasible disassembly plan found by a specific disassembly planner such as BurrTools [2013]. In contrast, we define the level of difficulty in a more strict way as the *minimal* number of moves to take out the first subassembly, which is intrinsic to the puzzle. Moreover, we develop a new graph-based disassembly planner that is able to compute this intrinsic level of difficulty and a computational framework that can construct the geometry of puzzle pieces to achieve the level of difficulty. Due to this reason, our approach can create high-level interlocking puzzles much more efficiently and flexibly, and generate results that cannot be achieved by the state-of-the-art approaches; see Section 7 for a quantitative comparison with [Gontier 2020].

Assembly planning. The goal of assembly planning is to find a sequence of operations to assemble the parts (i.e., *assembly sequencing* [Jiménez 2013]), and determine the motions that insert each part into the assembly (i.e., *assembly path planning* [Ghandi and Masehian 2015]). A bijection usually exists between assembly planning and disassembly planning [Halperin et al. 2000]. Hence, a common strategy to assembly planning is assembly-by-disassembly, where an assembly plan is obtained by computing a disassembly plan and then reversing its order and path.

To address the assembly sequencing problem, a number of data structures have been proposed to enumerate all possible assembly sequences, including Bourjault tree [Bourjault 1984], directed graph of assembly states [Fazio and Whitney 1987], and And/Or graph [Mello and Sanderson 1990]; readers are referred to the surveys [Jiménez 2013; Wolter 1991] for more details. All these data structures assume monotone assembly plans and cannot represent assembly states with intermediate placements of component parts. We address this issue by proposing a new graph data structure augmented with spatial information of the assembly such that it can enumerate all non-monotone assembly plans for high-level interlocking puzzles.

In the literature, there are very few works that deal with non-monotone assembly planning as pointed out in [Masehian and Ghandi 2020]. Tsao and Wolter [1993] proposed a method to generate a feasible non-monotone and non-linear assembly plan by assuming that intermediate states are given as input. Le et al. [2009] searched for a feasible non-monotone and linear disassembly plan by extending a sampling-based path planner. Masehian and Ghandi [2020] proposed a planner/replanner for monotone and non-monotone assembly planning, with advantages of supporting obstacles in the workspace and allowing translational and rotational movements of paths. Later, this approach was extended to support non-monotone assembly planning with both rigid and flexible parts [Masehian and Ghandi 2021]. All these existing approaches aim to find a feasible non-monotone (dis)assembly plan, making them inapplicable to our problem of finding an optimal non-monotone disassembly plan that requires a minimal number of moves to take out the first subassembly.

In the graphics community, (dis)assembly planning is typically formulated as an optimization problem to find a desired (dis)assembly plan that maximizes certain objectives. For example, the objective can be visibility of parts for creating visual assembly instructions [Agrawala et al. 2003], stability of incomplete assemblies for

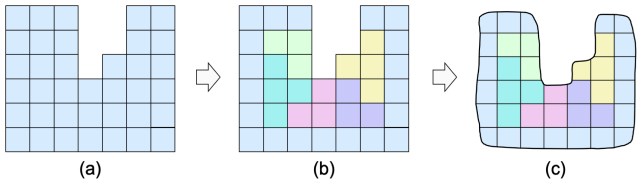

Fig. 3. Our approach takes (a) a voxelized shape as an input and partitions it to generate (b) a 6-piece level-6 interlocking puzzle (see its disassembly plan in Figure 4). The geometry of each voxelized puzzle piece can be further processed to obtain (c) a puzzle with smooth appearance.

illustration [Guo et al. 2013; Kerbl et al. 2015] and physical construction [Deuss et al. 2014]. Please refer to the survey [Wang et al. 2021] for details.

Assembly-aware design. Assembly-aware design varies the geometry of assemblies to enable desirable (dis)assembly plans, aiming for simplifying the physical (dis)assembly process. Desai et al. [2018] designed electromechanical devices that require only translational motion for parts assembly while Kao et al. [2017] designed masonry shell structures that require significantly fewer supports for physical construction. Our design of high-level interlocking puzzles follows the spirit of this design paradigm. However, rather than simplifying the (dis)assembly process, our goal is to complicate the (dis)assembly process of puzzles such that finding a (dis)assembly plan of the puzzles becomes an intriguing gaming process.

3 PROBLEM FORMULATION

Our input is a voxelized shape; see Figure 3(a). Users should also specify a target number of puzzle pieces K and a desirable level of difficulty L, where $L > 1$ since we focus on high-level interlocking puzzles. Our goal is to generate a K-piece level-L interlocking puzzle by partitioning the input voxelized shape into K puzzle pieces; see Figure 3(b). In case users prefer a puzzle with smooth appearance, we allow post-processing on the geometry of each voxelized puzzle piece to refine its appearance while preserving its structural soundness; see Figure 3(c).

Level of difficulty. Following the definition in [IBM Research 1997], we define the level of difficulty as follows:

> The level of an interlocking puzzle is the number of moves needed to remove the first piece or pieces, where a move is counted as one irregardless of how far a piece is moved in one direction.

Since we assume translational-only motion for disassembly, moving a piece is equivalent to translating a piece in our paper. Moving a piece in one direction and then immediately in another is considered as two moves; see Figure 2(b&c). The move to remove the piece is counted for the level also. Moving two or more pieces in the same direction simultaneously is counted as one move; see Figure 2(i). Given an interlocking puzzle, there may exist different ways to take out the first subassembly. We call these partial disassembly plans *kernel disassembly plans* and denote them as $\{D_i\}$. For each kernel disassembly plan D_i, we denote the number of moves to take out the first subassembly as $N(\ D_i\ )$. We define the interlocking puzzle's *exact level of difficulty* as

$$L_{\text{exact}} = \min_i N(\ D_i\ ) \tag{1}$$

Note that our definition of level of difficulty is unique and intrinsic to the puzzle, compared with the level computed by existing tools like Burr Tools [Röver 2013] that depends on the employed disassembly planner.

Design requirements. Given the user input, our designed puzzles should satisfy the following requirements:

(1) *Fabricability.* Each generated puzzle piece should be a single piece of connected geometry [1] that can be fabricated.
(2) *Puzzle piece size.* All the puzzle pieces should have similar sizes (i.e., similar number of voxels) to avoid fragmented pieces.
(3) *Level of difficulty L.* There should exist at least one disassembly plan that takes out the first subassembly with L moves. And there should not exist any disassembly plan that takes out the first subassembly with fewer than L moves.
(4) *Disassemblability.* The puzzle can be completely disassembled into individual puzzle pieces.

In case the input voxelized shape is convex, we can only generate level-1 interlocking puzzles since any movable puzzle piece can be directly removed; see Figure 2(a). To resolve this issue, we allow users to create small holes inside the convex shape by introducing a few hole voxels; see Figure 2(h) for an example. The purpose of these hole voxels is to enable intermediate moves (yet not removal) of the puzzle pieces.

Overview of our approach. In Section 4, we propose a disassembly planner that uses a rooted graph to represent all possible valid configurations of the puzzle as well as transitions among these configurations, until the first subassembly is taken out. To compute the exact level of difficulty, our planner finds a path with the shortest length from the initial puzzle state (i.e., root node) to any state where a single subassembly has been taken out. We also extend our planner to check whether a given puzzle can be disassembled into individual pieces.

In Section 5, we propose a computational approach to design high-level interlocking puzzles with voxelized shape. Our approach consists of two key components: an iterative design framework that ensures the generated puzzles satisfy the design requirements, and an algorithm to construct the geometry of each puzzle piece guided by the disassembly planer.

In Section 6, we introduce methods to extend our design approach for generating high-level interlocking puzzles with smooth appearance and structurally sound pieces. The idea is to formulate and solve a shape optimization problem to ensure that a sufficiently large subvolume of each voxel is covered by the optimized shape. By this, we can generate puzzle pieces with smooth appearance by simply performing CSG intersection between each voxelized puzzle piece and the optimized shape.

[1] A piece of connected geometry means that each voxel has at least one face-face contact with its neighbours to ensure structural soundness of the puzzle piece.

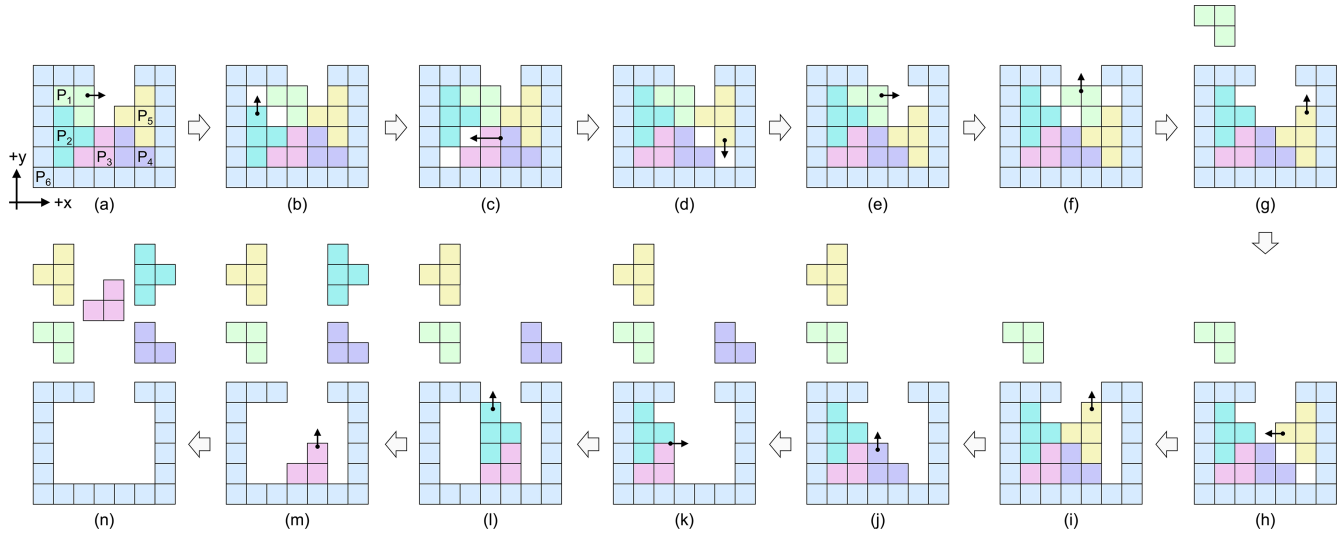

Fig. 4. Disassemble a 6-piece level-6 puzzle using a non-monotone and non-linear plan. The kernel disassembly plan is shown in (a-g) while the complete disassembly plan is shown in (a-n). In (g-h), we show disassembled puzzle pieces on top of the puzzle and adjust their positions to avoid overlap.

4 DISASSEMBLY PLANNER

The purpose of our disassembly planner is twofold. First, it should be able to compute the exact level of difficulty for a given interlocking puzzle (Section 4.2). Second, it should be able to identify if the puzzle can be disassembled into individual pieces (Section 4.3). To facilitate understanding of our approach, we first define a set of relevant concepts in Section 4.1.

4.1 Definitions

Given an interlocking puzzle $\mathbf{P}$, we denote its pieces as $\{P_1, ..., P_K\}$, $K \geq 3$, where K is the number of pieces in the puzzle. We assume that each puzzle piece is represented as a polycube, and the whole puzzle forms a voxelized shape.

To disassemble the puzzle, we assume that each puzzle piece can only translate along one of the three major axes following a certain order. Denote the side length of a voxel as μ. We call that a translation of a puzzle piece along one major axis for a distance $d = h \cdot \mu$ as a translation of h *steps*, where $h \geq 1$ and $h \in \mathbb{Z}$. We only consider these discrete translations for disassembling the puzzle pieces, due to the discrete nature of the voxelized shape.

State. A state for a puzzle piece P_i is defined as either the piece's initial position or other positions induced by a set of operations. We represent a puzzle piece P_i's state s_i using the displacement from its initial position. Hence, the initial state of each P_i is always $s_i = (0, 0, 0)$; see Figure 4(a). The state s_i consists of integers only due to the discrete nature of the voxelized shape. For example, the state of P_1 in Figure 4(b) is $(1, 0, 0)$ since it translates along $+x$ for one step from its initial state. We introduce the infinity state, denoted as ∞, to represent the state of a piece that is disassembled such as P_1 in Figure 4(g).

Operation. We define a disassembly operation for a puzzle piece as a change of state by translating along one of the major axes for one or multiple steps. That is, for each puzzle piece P_i, an operation is denoted by four variables $o_l = (s_i^u, s_i^v, d_j, h)$, where s_i^u is the source state that P_i moves from, s_i^v the destination state that P_i moves to, $d_j \in \{-x, +x, -y, +y, -z, +z\}$ is the moving direction of P_i, and h is the number of moving steps. We classify disassembly operations into the following two types, i.e. temporary operations and removal operations. A temporary operation is defined as an operation that moves a puzzle piece from a non-infinity state to another non-infinity state (e.g., moving P_1 along $+x$ in Figure 4(e) to reach the state in Figure 4(f)) whereas a removal operation moves a puzzle piece from a non-infinity state to the infinity state (e.g., moving P_1 along $+y$ in Figure 4(f) to remove it).

Move. In order to support non-linear disassembly planning, we define a move m_i to be a non-empty set of collision-free operations where the associated puzzle pieces are moved simultaneously along the same direction for the same distance; see the move of P_3 and P_4 along $-x$ in Figure 4(c). Obviously, a move is just a generalization of an operation from a single puzzle piece to a subset of puzzle pieces. Here, we require that the subset of puzzle pieces have to contact each other to form a connected piece of geometry. Such subset of puzzle pieces is called a *subassembly*, denoted as $\mathbf{S}_j$. Each single puzzle piece is considered as a special case of a subassembly.

Configuration. We define a puzzle configuration as a set of puzzle pieces together with their states, i.e., $C = \{(P_1, s_1), ..., (P_K, s_K)\}$. A configuration is valid if there is no overlap among the puzzle pieces in the configuration (i.e., collision-free). According to the states of the puzzle pieces, we classify a configuration $\mathbf{C}$ into three types:

(1) *Full configuration.* In a full configuration, the state $s_i = \infty$ for none of the K puzzle pieces; see Figure 4(a-f).
(2) *Partial configuration.* In a partial configuration, the state $s_i = \infty$ for k puzzle pieces, where $1 \leq k \leq K - 2$, meaning that k puzzle pieces have been disassembled; see Figure 4(g-m);

Algorithm 1 Algorithm to build a kernel disassembly graph G for a given interlocking puzzle **P**.

```
1:  function BuildKernelDisassemblyGraph(P)
2:      G = (V, E) ← ∅
3:      let C_1 be the initial puzzle configuration
4:      mark C_1 as the root node
5:      V.push_back( C_1 )
6:      let Q be queue
7:      Q.enqueue( C_1 )
8:      mark C_1 as unvisited
9:      while Q is not empty do
10:         C = Q.dequeue( )
11:         if C has been visited then
12:             continue
13:         if C is not a full configuration then
14:             mark C as a target node
15:         else
16:             C_neighbor = ComputeNeighborConfigs( C )
17:             for each C_k in the list C_neighbor do
18:                 if C_k ∈ V then
19:                     if (C, C_k) ∉ E then
20:                         E.push_back( (C, C_k) )
21:                 else
22:                     V.push_back( C_k )
23:                     E.push_back( (C, C_k) )
24:                     mark C_k as unvisited
25:                     Q.enqueue( C_k )
26:         mark C as visited
        return G
```

(3) *Final configuration.* In a final configuration, the state $s_i = \infty$ for at least $K - 1$ puzzle pieces; i.e., the puzzle has been completely disassembled into individual puzzle pieces; see Figure 4(n);

Kernel disassembly plan. We define a kernel disassembly plan $D_{\text{kern}} =< m_1, m_2, ..., m_l >$ as an ordered sequence of moves to take out the first subassembly, where l is the number of moves in D_{kern}; see Figure 4(a-g). This kernel disassembly plan can also be represented as a set of configurations of the puzzle, i.e., $D_{\text{kern}} =< C_1, C_2, ..., C_{l+1} >$, where C_1 is the initial puzzle configuration and C_{j+1} is the configuration obtained by applying move m_j onto the configuration C_j. We require that each C_j, where $1 \leq j \leq l$, is a full configuration while C_{l+1} is a partial configuration with exactly one removed subassembly.

Complete disassembly plan. We define a complete disassembly plan $D_{\text{comp}} =< m_1, m_2, ..., m_l, ..., m_q >$ as an ordered sequence of moves to disassemble the puzzle into individual pieces, where q is the number of moves in D_{comp}; see Figure 4. Similarly, the complete disassembly plan can be represented as a set of configurations of the puzzle, i.e., $D_{\text{comp}} =< C_1, C_2, ..., C_{l+1}, ..., C_{q+1} >$, where C_{q+1} is the final configuration. From the definition, we can see that there exists $l < q$ such that the first l moves in a complete disassembly plan form a kernel disassembly plan.

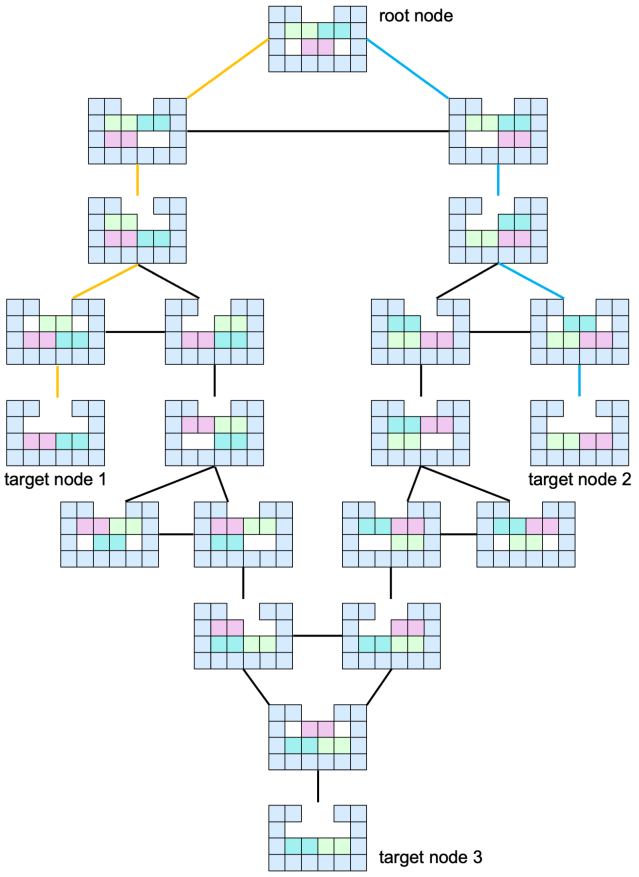

Fig. 5. The kernel disassembly graph of a 4-piece level-4 interlocking puzzle. The graph has three target nodes, and the exact level (i.e., 4) of the puzzle is defined by the shortest path from the root node to the target node 1 or 2 (the path is colored in orange or cyan respectively).

4.2 Computing Level of Difficulty

To compute the level of difficulty, we have to enumerate all possible kernel disassembly plans to take out the first subassembly; see Equation 1. However, directly enumerating all these plans has significant redundancy in computation since many plans share the same configurations with different orders. To avoid the ordering problem [Wu et al. 2019], our idea is to enumerate all the valid configurations of the puzzle as well as valid transitions among these configurations instead. To this end, we propose a rooted graph data structure called *kernel disassembly graph* to encode all possible kernel disassembly plans, in which each node represents a puzzle configuration and each edge represents a move of a subassembly. A kernel disassembly graph is an undirected graph since a move is bidirectional according to its definition; see Figure 5 for a simple example.

In a kernel disassembly graph, the root node is the initial puzzle configuration C_1, and nodes with one subassembly removed are called target nodes. All the nodes except the target nodes in the graph are full configurations. A kernel disassembly plan is a path from the root node to one target node in the graph, where the length of the path is the number of moves to take out the first subassembly.

Algorithm 2 Algorithm to compute all possible configurations that can be achieved by performing one move on a configuration C.

```
function ComputeNeighborConfigs(C)
    vector C_next ← ∅
    for each subassembly S with ≤ ⌈K/2⌉ pieces in C do
        for each major axis d ∈ {−x, +x, −y, +y, −z. + z} do
            if S is movable along d then
                Compute the max. number of movable steps L
                if L = ∞ then
                    C_k ← C
                    Remove S in C_k
                    C_next.append( C_k )
                    continue
                else
                    for 1 ≤ i ≤ L do
                        C_k ← C
                        Move S along d for i steps in C_k
                        C_next.append( C_k )
                        i + +
    return C_next
```

Algorithm 3 Algorithm to generate a complete disassembly plan D_{comp} for a given puzzle $\mathbf{P}$.

```
function DisassemblePuzzle(P, D_comp)
    if P consists of a single piece then
        return true
    { D_kern, S_remv, P_rema } = RemvSubassembly( P )
    if D_kern != NULL then
        D_comp.append( D_kern )
        DisassemblePuzzle( S_remv, D_comp )
        DisassemblePuzzle( P_rema, D_comp )
    else if P has more than one piece then
        return false
     return true
```

To compute the exact level of difficulty, we simply need to compute a shortest path from the root node to each target node, choose a path with the shortest length among all the shortest paths, and count the number of edges in the path; see again Figure 5.

To build the kernel disassembly graph, we propose an algorithm based on breadth-first search; see Algorithm 1. Starting from the root node, this algorithm builds the graph by iteratively inserting new nodes (i.e., neighboring nodes) that can be reached by a single move from a current node in the graph. To compute these neighboring nodes, we identify all possible movable subassemblies in the current node C as well as their moving directions, and compute the longest movable distance along each direction for each subassembly. Due to the relativity of motion, we only need to perform this mobility computation for subassemblies with less than or equal to $\lceil K/2 \rceil$ pieces. Each neighbor of the node C is computed by applying a possible move to the configuration C; see Algorithm 2. A subassembly is removable in the configuration C if its longest movable distance is infinity. Applying this move to the configuration C will lead to a target node in the graph. This graph expanding process terminates when no new node or edge can be inserted in the graph.

4.3 Disassembly Planning

A given puzzle is possible to be not disassemblable, which can be classified into three cases: 1) the whole puzzle is deadlocking; 2) the puzzle is deadlocking after taking out a few puzzle pieces; and 3) at least one removed subassembly is deadlocking; see Figure 6 for examples. Algorithm 1 can only identify the first case of deadlocking (i.e., no target node in the graph) but not the other two cases. Hence, we need to extend the algorithm to check if a given puzzle can be disassembled into individual puzzle pieces, which is known to be an NP-hard problem [Kavraki et al. 1993].

To speed up the planning process, our algorithm aims to find a feasible (i.e., collision-free) complete disassembly plan instead of enumerating all possible complete disassembly plans; see Algorithm 3. Hence, our algorithm cannot guarantee that the puzzle is not disassemblable if it does not find a complete disassembly plan. In detail, we first modify Algorithm 1 to find a feasible kernel disassembly plan that removes a single subassembly from a puzzle $\mathbf{P}$ by terminating the graph expanding process once it finds a target node; see `RemvSusbassembly(P)` in Algorithm 3. Our disassembly planning algorithm calls this function recursively for both the removed subassembly $\mathbf{S}_{\text{remv}}$ and the remaining puzzle $\mathbf{P}_{\text{rema}}$. This recursion terminates when $\mathbf{P}_{\text{rema}}$ and each $\mathbf{S}_{\text{remv}}$ consist of a single puzzle piece respectively (i.e., $\mathbf{P}$ is disassemblable) or when there is no subassembly that can be taken out from $\mathbf{P}_{\text{rema}}$ or $\mathbf{S}_{\text{remv}}$ (i.e., $\mathbf{P}$ is not disassemblable).

Besides the first removed subassembly, it may also require multiple moves to take out some of the subsequent subassemblies. For example, in Figure 4, it takes 6 moves to take out the firstly removed piece P_1 and 3 moves to take out the secondly removed piece P_5. An alternative way to measure an interlocking puzzle's level of difficulty is to use the total number of moves to completely disassemble the puzzle into individual pieces, denoted as L_{total}. However, since our disassembly planner can only find a feasible complete disassembly plan due to the huge search space, our computed L_{total} cannot be guaranteed to be the smallest total number of moves to disassemble the puzzle.

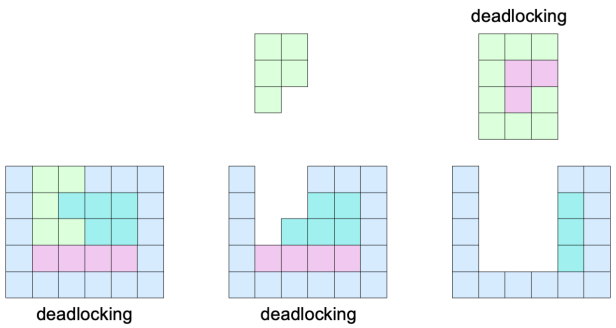

Fig. 6. Three cases of deadlocking puzzles. From left to right, the whole puzzle, the puzzle after removing the green piece, and the removed subassembly, are deadlocking.

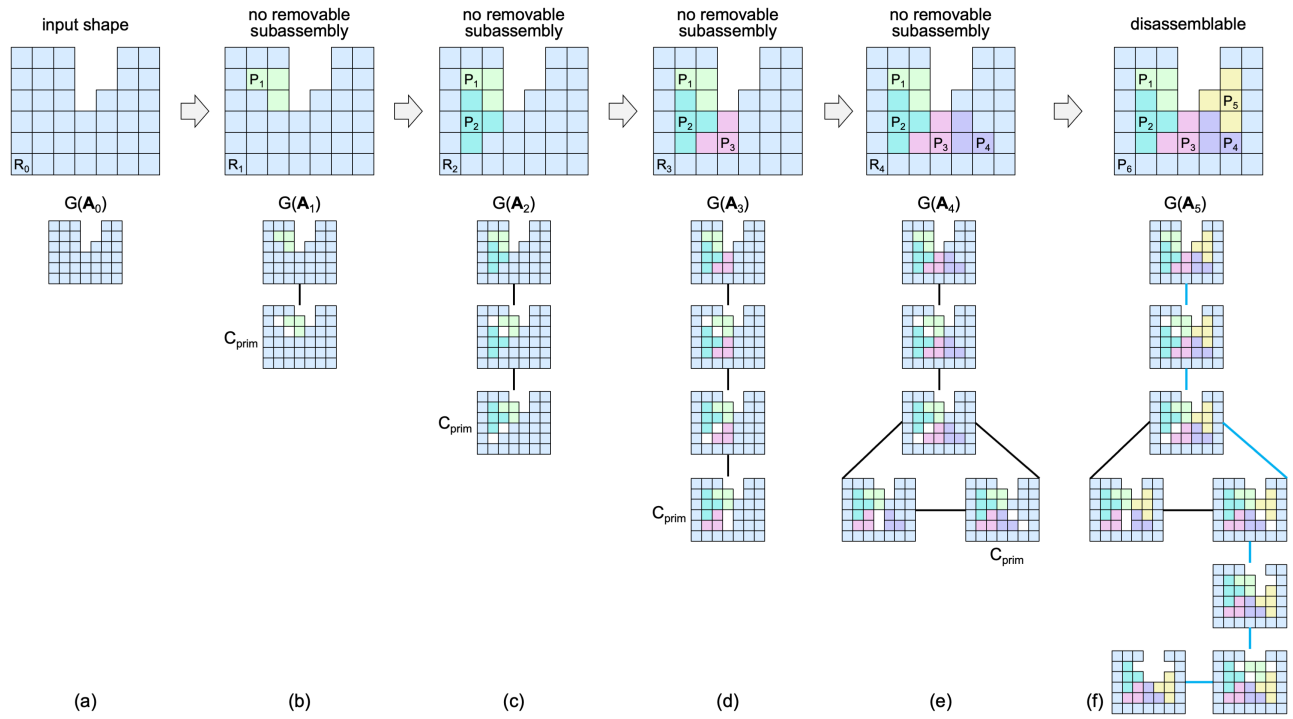

Fig. 7. Overview of our design approach. (a) Taking a voxelized shape as an input, (b-f) we generate the geometry of each puzzle piece iteratively by partitioning the shape, during which we build (bottom) a kernel disassembly graph for (top) each intermediate puzzle. To increase the level of difficulty, we require that (b-e) each intermediate puzzle should not have any removable subassembly and (f) only the resulting puzzle is disassemblable when the last two puzzle pieces P_5 and P_6 are constructed. The shortest path in the graph to take out the first subassembly (i.e., P_1) is colored in blue.

5 PUZZLE DESIGN APPROACH

To address the puzzle design problem formulated in Section 3, a straightforward approach would be a trial-and-error approach that iterates between randomly assigning piece IDs (from 1 to N) to each voxel in the input shape and checking whether the resulting puzzle satisfies the requirements in Section 3. However, this approach is very inefficient and hard to generate a desirable result since each puzzle piece can be easily disconnected and the puzzle can be easily non-interlocking or non-disassemblable, especially when the input shape has a large number of voxels; see Section 7 for the complexity analysis of our puzzle design problem.

In this section, we propose a computational approach to design a K-piece level-L interlocking puzzle by constructing the geometry of each puzzle piece iteratively; see Figure 7. Section 5.1 introduces our computational framework as well as a set of requirements on constructing each puzzle piece. Section 5.2 presents an algorithm that constructs the geometry of each puzzle piece to satisfy the requirements in Section 5.1.

5.1 Computational Framework

Given the input voxelized shape denoted as R_0, we iteratively construct the geometry of each puzzle piece one by one; see Figure 7 for an example. This forms a sequence of constructed puzzle pieces, $P_1, P_2, ..., P_{K-1}, P_K$:

$$[R_0] \rightarrow [P_1, R_1] \rightarrow [P_1, P_2, R_2] \rightarrow ... \rightarrow [P_1, ...P_{K-1}, R_{K-1}]$$

where R_i, $1 \leq i \leq K-1$, is the remaining part of the shape and $R_{K-1} = P_K$ is the last puzzle piece. Here we denote each intermediate assembly $[P_1, ..., P_i, R_i]$ as $\mathbf{A}_i$ $(0 \leq i \leq K-1)$, and its kernel disassembly graph as $G(\mathbf{A}_i)$.

To design a high-level interlocking puzzle, our idea is that the construction of each puzzle piece has to increase or at least preserve the potential level of difficulty for the resulting puzzle. To this end, we require that there is no removable subassembly in any of the intermediate puzzles $\mathbf{A}_i$, $1 \leq i \leq K-2$; see Figure 7(b-e). In other words, each node in each kernel disassembly graph $G(\mathbf{A}_i)$, $1 \leq i \leq K-2$, should be a full puzzle configuration. And only the resulting puzzle $\mathbf{P} = \mathbf{A}_{K-1}$ is disassemblable after we construct the last two puzzle pieces by decomposing R_{K-2} into P_{K-1} and P_K; see Figure 7(f). Otherwise, the level of difficulty of the resulting puzzle will be the same as or smaller than that of the first intermediate assembly $\mathbf{A}_i$ with removable subassemblies, no matter how we construct the geometry for the subsequent puzzle pieces. To increase the level of difficulty, we further require that each kernel disassembly graph $G(\mathbf{A}_i)$ should have as many nodes as possible, especially those far away from the root node.

To implement the above idea, we propose the following requirements when decomposing R_{i-1} into P_i and R_i, where $1 \leq i \leq K-1$:

(i) *Connected geometry.* The geometry of P_i and R_i should be connected respectively, making them fabricable.

(ii) *Puzzle piece size.* The number of voxels of P_i should be within the range $[(1-\delta)\lfloor M/K \rfloor, (1+\delta)\lfloor M/K \rfloor]$, where M is the total

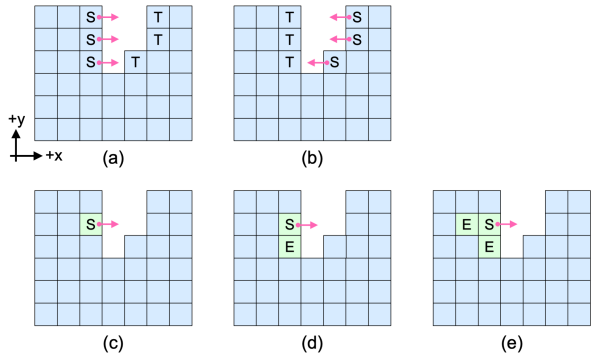

Fig. 8. Constructing the first puzzle piece P_1. (a&b) Candidates of seed voxels (marked as S) for $d_1 = +x$ and $d_1 = -x$ respectively, where there should exist voxels (marked as T) that stop P_1's movement along d_1. (c) Choose a seed voxel for the first puzzle piece and (d&e) incrementally expand the piece by adding voxels (marked as E) one by one.

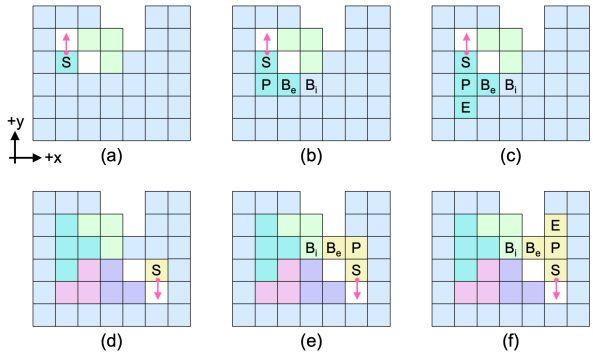

Fig. 9. (Top) Construct P_2 in the configuration C_{prim} in Figure 7(b). (Bottom) Construct P_5 in the configuration C_{prim} in Figure 7(e). (a&d) Select a moving direction d_i and a seed voxel S. (b&e) Select a pair of blockee and blocking voxels (marked as B_e and B_i respectively) and connect the seed voxel S with the blockee voxel B_e using a shortest path (voxels on the path are marked as P). (c&f) Expand the puzzle piece.

number of voxels in the input shape R_0 and $\delta \in [0, 1]$ is a user specified parameter.

(iii) *Movable puzzle piece.* P_i should be movable in a configuration that is furthest away from the root configuration in $G(\mathbf{A}_{i-1})$, aiming to extend the graph in a depth-first manner.

(iv) *No removable subassembly in* $\mathbf{A}_i$, $1 \le i \le K-2$. There is no removable subassembly in each intermediate puzzle $\mathbf{A}_i$ after constructing P_i, where $1 \le i \le K-2$.

(v) *Disassemblable puzzle* $\mathbf{A}_{K-1}$. The resulting puzzle $\mathbf{A}_{K-1}$ becomes disassemblable after constructing P_{K-1}.

Our computational framework guarantees that the resulting puzzle $\mathbf{A}_{K-1}$ satisfies the fabricability, puzzle piece size, and disassemblability requirements in Section 3. Moreover, our framework aims to generate an interlocking puzzle with an as-high-as-possible level of difficulty, although it does not have exact control over the level of difficulty of the resulting puzzle. To this end, we allow some modification operations on the resulting puzzle to satisfy the level of difficulty requirement in Section 3.

5.2 Puzzle Piece Construction

We propose an approach to construct each puzzle piece P_i, $1 \le i \le K-1$, to satisfy the requirements in Section 5.1. We first present our approach to construct the first piece P_1 and then the other pieces P_i, $2 \le i \le K-1$. Lastly, we introduce the modification operations on the pieces $\{P_i\}$ to achieve the user-specified level of difficulty L.

Constructing P_1. Constructing the first puzzle piece P_1 is relatively simple since the kernel disassembly graph $G(\mathbf{A}_0)$ only has a single node, which is the input shape R_0. According to the requirements in Section 5.1, P_1 should be movable but not removable in the input shape R_0. Moreover, P_1 should be movable along a single direction denoted as d_1 in R_0, aiming to make the resulting puzzle more stable. We construct P_1 with the following steps:

i) Pick the moving direction d_1. We first identify the set of non-height-field directions for the input shape R_0; e.g., the set should be $\{+x, -x\}$ for the input shape in Figure 7. We randomly choose one direction in the set as P_1's moving direction d_1. Height-field directions cannot be selected since they will make P_1 removable along the direction.

ii) Pick a seed voxel. For a selected moving direction d_1, a seed voxel should not contact any voxel along d_1, to ensure mobility of P_1 along d_1. To ensure that P_1 is not removable along d_1, there should exist some voxels that stop the movement of P_1 along d_1. We identify all voxels satisfy the two conditions; see Figure 8(a&b) for examples. We randomly choose one voxel from the set as a seed voxel; see Figure 8(c).

iii) Ensure blocking. If the seed voxel is also movable along a direction that is not d_1, we prevent such motion by identifying a pair of blocking and blockee voxels and connecting the seed voxel with the blockee voxel using a shortest path [Song et al. 2012].

iv) Expand P_1. Since P_1 usually has a few voxels at this moment, the goal of this step is to augment it with more voxels to balance the size of the puzzle piece. To this end, we add voxels one by one to P_1, without violating the mobility and blocking conditions that have been satisfied; see Figure 8(d&e).

Constructing P_i, $2 \le i \le K-1$. Constructing the subsequent puzzle piece P_i is more complex since it has to satisfy the requirements for all the configurations in $G(\mathbf{A}_{i-1})$. To increase the level of difficulty, we identify configurations in $G(\mathbf{A}_{i-1})$ that are furthest away from the root node in $G(\mathbf{A}_{i-1})$. We randomly choose one as a primary configuration for constructing P_i, denoted as C_{prim}; see Figure 7(b-e). Our idea is to make P_i movable but not removable in the configuration C_{prim} of $G(\mathbf{A}_{i-1})$ such that we can create new configurations in $G(\mathbf{A}_i)$ that are even further away from the root node than C_{prim} in $G(\mathbf{A}_{i-1})$.

i) Pick the moving direction d_i *in configuration* C_{prim}. We identify the set of non-height-field directions for the assembly $\mathbf{A}_{i-1}$ at configuration C_{prim}, and randomly choose one direction in the set as P_i's moving direction d_i; see Figure 9(a&d).

ii) Pick a seed voxel in configuration C_{prim}. A seed voxel is selected such that P_i is movable but not removable along direction d_i in the

Algorithm 4 Algorithm to modify a puzzle **P** to increase its level of difficulty to L.

```
function ModifyPuzzle(P)
    for m=0; m<IterNum; m++ do
        randomly select a voxel V_k in P using reachability
        randomly select a neighboring puzzle piece P_j of V_k
        let P_i be the puzzle piece that has V_k
        assign V_k from P_i to P_j
        let P̄ be the modified puzzle
        if P_i in P̄ is not connected then
            continue
        if P̄ is not disassemblable then
            continue
        if L_exact(P̄) == L then return P̄
        if (L_exact(P̄) > L_exact(P)) || ((L_exact(P̄) == L_exact(P)) &&
    (L_total(P̄) > L_total(P))) then
            P ← P̄
    return NULL
```

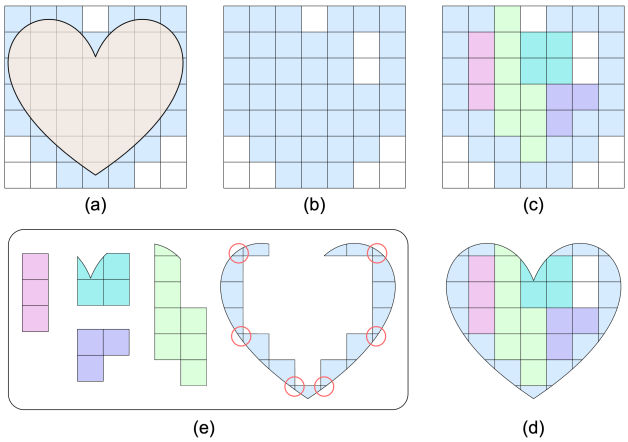

Fig. 10. (a) Voxelizing a given smooth shape. (b) Taking the voxelized shape (with two hole voxels) as an input, we generate a (c) 5-piece level-2 interlocking puzzle by using our design approach in Section 5. (d) A puzzle with smooth appearance is obtained by performing CSG intersection between each voxelized puzzle piece in (c) and the input shape in (a). (e) However, the generated puzzle pieces are possible to be structurally weak for fabrication and playing (see red circles).

primary configuration C_{prim} using the same approach for picking a seed voxel for P_1.

iii) Ensure blocking in all configurations in $G(\mathbf{A}_{i-1})$. If the seed voxel is movable along a direction that is not d_1 in C_{prim} or movable along any direction in other nodes in $G(\mathbf{A}_{i-1})$, we will summarize all these unwanted mobilities, choose a minimal number of pairs of blocking and blockee voxels, and connect the seed voxel with each blockee voxel using a shortest path to get rid of the mobilities; see Figure 9(b&e).

iv) Expand P_i. We expand P_i by adding voxels one by one to P_i, without violating the mobility and blocking conditions that have been satisfied for any configuration in $G(\mathbf{A}_{i-1})$; see Figure 9(c&f).

The above puzzle piece construction process may not be always successful. When it fails, our approach backtracks until all the puzzle pieces can be successfully constructed and disassembled. We compute the level of difficulty of our generated puzzle by running the disassembly planner in Section 4. In case that the generated puzzle's level of difficulty is different from the user-specified level L, we will re-generate another puzzle design by repeating the random construction process of the puzzle pieces. Our approach terminates when the puzzle's level of difficulty is the same as the user-specified level L or the computation time exceeds a user-specified threshold. In practice, we find that our approach is efficient when the user-specified level L is not that large. However, when L is large, our approach may fail to generate such puzzles within a user-specified time threshold. To address this limitation, we introduce additional modification operations on a puzzle generated by our approach, aiming to increase its level of difficulty to the user-specified L.

Modifying $\{P_i\}$, $1 \le i \le K$. We found that an interlocking puzzle's level of difficulty is possible to be increased by a slight modification on the puzzle geometry in our experiments. Inspired by this observation, we perform the slight puzzle geometry modification iteratively using Algorithm 4 to increase the level of difficulty. Our algorithm consists of the following steps: 1) randomly choose a voxel on the puzzle according to its reachability [Song et al. 2012] (i.e., we prefer to choose a voxel with fewer number of neighbors); 2) assign the voxel to a neighboring puzzle piece that is randomly selected; 3) compute the modified puzzle's level of difficulty L_{exact} and total number of moves L_{total}; and 4) update the puzzle geometry if the modification leads to a larger L_{exact} and/or L_{total}. The process terminates when finding a level-L interlocking puzzle or exceeding the maximum number of iterations.

6 SHAPE OPTIMIZATION AND VOXELIZATION

Our computational design approach in Section 5 can generate high-level interlocking puzzles with voxelized shape. In this section, we will extend our computational design approach to support generating puzzles with smooth appearance. To this end, a straightforward approach is to directly perform a CSG intersection operation between each voxelized puzzle piece and the input smooth shape; see Figure 10(a-d). However, this simple approach may result in structurally weak puzzle pieces that can easily break during fabrication or playing; see Figure 10(e). Such puzzle pieces typically include voxels that contain only a tiny part of the input smooth shape, called *problematic voxels*.

To address this issue, our idea is to minimize the number of such problematic voxels by allowing slight deformation on the input smooth shape during the voxelization. Then, we take the voxelized shape without the problematic voxels to generate a high-level interlocking puzzle, which guarantees the structural soundness of each puzzle piece. In the end, we attach the tiny shape contained in the problematic voxels (if any) back to the corresponding puzzle piece following the approach in [Song et al. 2015]. We formulate our problem of shape optimization for voxelization in Section 6.1 and then present a method to solve the problem in Section 6.2.

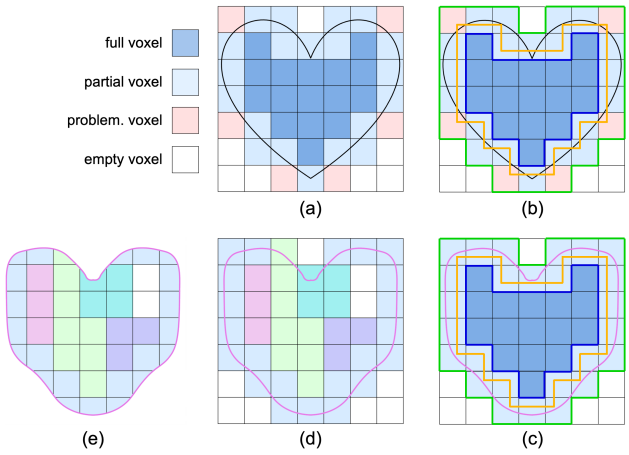

Fig. 11. (a) Classify voxels in a voxelized shape. (b) Compute a shell whose inner (in orange) and outer (in green) surfaces are obtained by offsetting the boundary surface (in dark blue) of the full voxels. (c) Optimize the input surface to minimize its distance to the shell, and thus to minimize the number of problematic voxels. (d&e) Refine the puzzle's appearance by using the optimized smooth surface (in purple).

6.1 Shape Optimization Problem

The input smooth shape is represented as a mesh surface $\mathbf{M}$ with vertices $\mathbf{V}$ and faces $\mathbf{F}$. Assuming the voxel size μ is specified by the user, we obtain an initial voxelized shape by voxelizing the mesh $\mathbf{M}$ with the voxel size μ [Nooruddin and Turk 2003]. We classify voxels in the voxelized shape into three classes according to the position of each voxel relative to the mesh $\mathbf{M}$: full voxel that is totally inside the mesh $\mathbf{M}$, empty voxel that is totally outside of the mesh $\mathbf{M}$, and partial voxel that intersects the mesh $\mathbf{M}$. We further identify problematic voxels as partial voxels that contain a tiny amount of local shape of $\mathbf{M}$; see Figure 11(a). In our experiments, problematic voxels are partial voxels with less than $0.1\mu^3$ volume filled.

The goal of our shape voxelization is to minimize the number of problematic voxels while preserving the input shape $\mathbf{M}$ as much as possible. Our search space includes: 1) a translational vector $\mathbf{t}$ that defines the position of the mesh $\mathbf{M}$ with respect to the voxelized shape; 2) a uniform scale factor w of the mesh $\mathbf{M}$; and 3) vertices $\mathbf{V}$ of the mesh $\mathbf{M}$. We formulate our shape voxelization problem as an optimization problem:

$$\min_{\mathbf{t},w,\mathbf{V}} E_{\texttt{voxel}}(\mathbf{t}, w, \mathbf{V}) \; + \; \lambda E_{\texttt{shape}}(\boldsymbol{V}) \tag{2}$$

where $E_{\texttt{voxel}}$ is the number of problematic voxels, $E_{\texttt{shape}}$ is the shape preservation energy, and λ is the weight for the energy $E_{\texttt{shape}}$. We define the energy $E_{\texttt{shape}}(\mathbf{V})$ as an as-rigid-as-possible shape preservation energy [Sorkine and Alexa 2007].

6.2 Optimization Solver

Solving the optimization problem in Equation 2 is challenging due to two reasons. First, computing the gradient of $E_{\texttt{voxel}}$ is complex, which typically involves differentiation on the CSG intersection operation between each voxel and the mesh $\mathbf{M}$. Second, the search space is large, and contains both the transformation $(\mathbf{t}, w)$ and geometry $\mathbf{V}$ of the input shape $\mathbf{M}$.

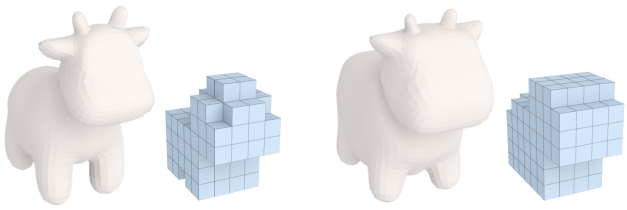

Fig. 12. A Cow (left) before and (right) after our shape optimization. The corresponding voxelized shape is also shown beside.

To address the first challenge, our observation is that the boundary surface $\mathbf{M}_{\text{full}}$ of the set of full voxels is a good approximation of the input surface $\mathbf{M}$; see Figure 11(a). Hence, we define a shell $\mathbf{S}$ whose outer and inner surfaces are obtained by offsetting the boundary surface $\mathbf{M}_{\text{full}}$ by μ and $a \cdot \mu$ ($0.5 \le a \le 0.9$ in our experiments) distance, respectively; see Figure 11(b). If the input mesh $\mathbf{M}$ can be optimized such that it is contained in the shell $\mathbf{S}$, then there is no problematic voxel since the local shape volume covered in each partial voxel is at least $(a \cdot \mu)^3$; see Figure 11(c). Moreover, the closer the mesh $\mathbf{M}$ is to the shell $\mathbf{S}$, the more likely there is a fewer number of problematic voxels. Hence, we define:

$$E_{\texttt{voxel}}(\boldsymbol{t}, w, \boldsymbol{V}) = \sum_{F_i \in \mathbf{F}} \left(\text{dist}(F_i(\boldsymbol{t}, w, \mathbf{V}),\ \mathbf{S}) \right)^2 \tag{3}$$

where F_i is a face of the mesh $\mathbf{M}$ and $\text{dist}(F_i, \mathbf{S})$ is the distance between the face F_i and the shell $\mathbf{S}$. When a face F_i is contained in the shell, $\text{dist}(F_i, \mathbf{S}) = 0$.

To address the second challenge, we use a two-stage approach to explore the search space effectively. First, the transformation stage fixes the vertex positions $\mathbf{V}$ and searches for an optimal transform $(\mathbf{t}, w)$ to minimize the energy $E_{\texttt{voxel}}$, during which we perform voxelization for each transformed mesh to compute the energy $E_{\texttt{voxel}}$. Since the transform $(\mathbf{t}, w)$ is only 4 degrees of freedom, we can uniformly sample the variables' space of $(\mathbf{t}, w)$ to find the optimal one. Then, the deformation stage fixes the mesh transformation $(\mathbf{t}, w)$ and deforms the input mesh $\mathbf{M}$ to minimize the energy of Equation 2, assuming the voxelization is fixed. We use the L-BFGS algorithm to solve the mesh deformation problem. We iterate between the shape transformation stage and shape deformation stage until the ratio between the number of problematic voxels and the total number of voxels cannot be further reduced.

Figure 12 shows an example before and after our shape optimization. It took our algorithm 30 minutes to reduce the problematic voxel ratio from 23.3% to 11.7%. Please refer to the supplementary material for details about our optimization solver.

7 RESULTS

We implemented our computational design tool in C++ and libigl [Jacobson et al. 2018] on a desktop computer with 3.6 GHz 8-Core Intel processor and 16 GB RAM. Our tool allows user control in several aspects (see Table 1):

- *Voxelization resolution.* Users can specify the input voxelized shape's resolution, typically fewer than 1000 voxels. Low-resolution voxelized shapes are preferred since they ensure that the move

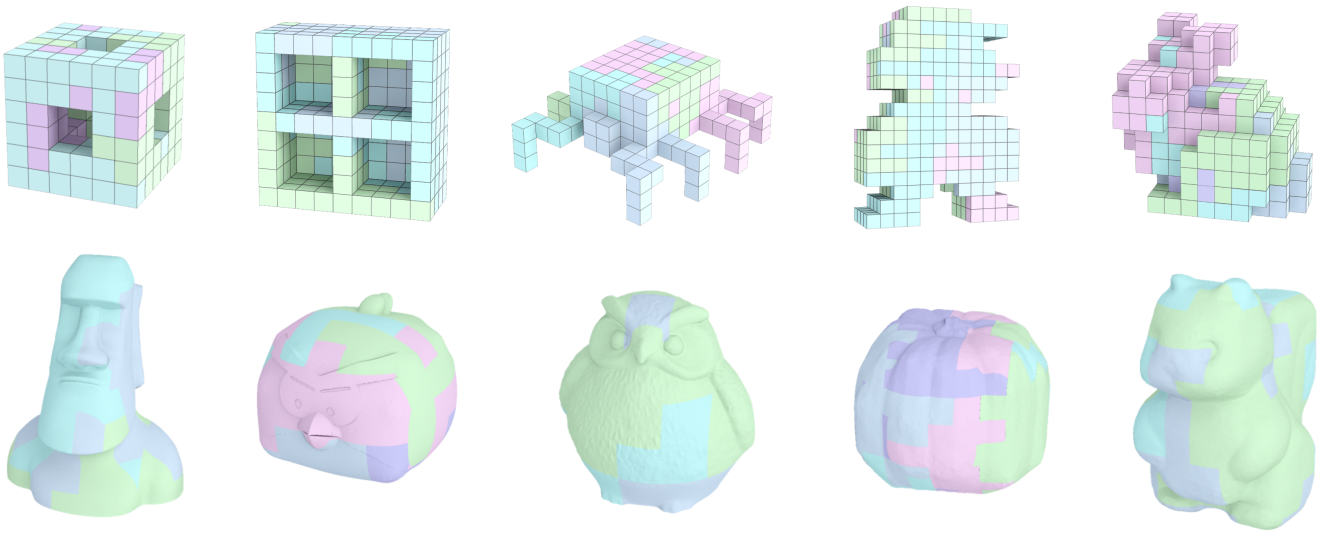

Fig. 13. High-level interlocking puzzles generated by our approach. From left to right and then top to bottom: Cube Frame, Shelf, Spider, Mario, Bunny, Moai, Angry Bird, Owl, Pumpkin, and Squirrel.

of each puzzle piece for disassembly is significant relative to the whole puzzle size.

- *Number of hole voxels E.* For convex input shapes such as Cube, hole voxels are needed to generate high-level interlocking puzzles. By default, our tool inserts a single hole voxel at the center of the shape. Users can override this by specifying the number of hole voxels E as well as their locations in the input shape.
- *Number of puzzle pieces K.* The number of puzzle pieces K is typically between 3 and 8.
- *Target level of difficulty L.* The target level of difficulty L is typically between 4 to 30. When L is too large, our tool may not be able to generate such a puzzle. In this case, our tool will output the puzzle whose level of difficulty is closest to L.

Results. Our design tool allows generating high-level interlocking puzzles with a variety of voxelized shapes and topologies, including Cube Frame with hollows, Shelf with four large cavities, Spider with elongated features, and Mario with a 2.5D shape; see Figure 13 (top). The variety of 3D shapes that can be represented by a low-resolution voxelization is limited. Thanks to our shape optimization, our tool can generate high-level interlocking puzzles with smooth appearance, which significantly extends the resulting puzzles' shape complexity and variety; see Figure 13 (bottom). Our tool can generate interlocking puzzles with a very high level of difficulty; see the 5-piece level-27 interlocking Cube in Figure 15. We refer to the accompanying video for the disassembly animation of the results. We provide the puzzle piece 3D models and the kernel disassembly graph of each result in the supplementary material.

Table 1 provides the statistics of all the results shown in the paper. To generate high-level interlocking puzzles efficiently, it is usually necessary to modify the puzzle pieces using Algorithm 4; see the second column from right in the table. For example, we could not generate a level-15 Shelf by running the puzzle piece construction algorithm for 24 hours. Instead, we were able to generate a level-15 Shelf within 1.23 hours by first generating a level-6 Shelf using the puzzle piece construction algorithm (0.95 hours) and then modifying the puzzle's geometry using Algorithm 4 (0.28 hours).

Table 1. Statistics of our results. The labels in 4th to 12th columns refer to the voxelization resolution, number of hole voxels E, number of puzzle pieces K, level of difficulty L, number of nodes (G_N), edges (G_E), and target nodes (G_T) in the kernel disassembly graph, whether the puzzle pieces are modified to improve the level of difficulty (Modify), and time for generating the result (excluding time for shape optimization).

Fig.	Model	Smooth Appearance	Resolution	E	K	L	G_N	G_E	G_T	Modify	Time (mins)
1	Cow	Yes	4x7x8	1	4	6	9	10	1	No	5.81
13	Cube Frame	No	6x6x6	0	3	9	65	89	18	Yes	2.67
	Shelf	No	9x9x4	0	3	15	55	109	2	Yes	74.06
	Spider	No	12x13x6	0	4	8	25	32	5	Yes	47.02
	Mario	No	12x16x4	0	4	8	22	32	3	Yes	52.44
	Bunny	No	11x10x8	0	5	7	15	17	3	Yes	17.77
	Moai	Yes	8x6x9	1	3	7	18	20	4	Yes	11.02
	Angry Bird	Yes	7x6x8	1	5	10	15	15	2	Yes	12.90
	Owl	Yes	5x5x5	1	3	7	8	7	1	Yes	6.75
	Pumpkin	Yes	9x9x9	1	5	9	11	11	1	Yes	13.77
	Squirrel	Yes	6x9x8	1	3	9	15	18	1	Yes	7.52
14	Cube	No	5x5x5	1	4	16	64	82	14	Yes	70.76
	Sofa	No	7x8x6	0	4	8	307	637	91	No	25.04
	Airplane	No	14x6x17	0	5	10	66	92	11	No	83.47
15	Cube	No	6x6x6	1	5	27	54	84	1	Yes	383.72

Complexity and performance. The complexity of our puzzle design problem is $O(K^N \cdot N^{2K})$, where K is the number of puzzle pieces and N is the number of voxels. For a given input shape, the total number of possible puzzle designs (including invalid ones) is K^N, since each voxel can be assigned to any puzzle piece. For each design, we need to compute its level of difficulty by building a kernel disassembly graph using a BFS-based algorithm with complexity $O(V + E)$, where V and E are the number of vertices and edges in the graph respectively. In the worst case, $V = N^K$ since each puzzle

Table 2. Comparing our approach with a baseline [Gontier 2020] for generating high-level interlocking Cubes with a single hole voxel at the center. The numbers in the table are the highest level of difficulty that can be achieved by both approaches, given the same amount of computation time (i.e., 12 hours).

	Cube_4x4x4_E1				Cube_5x5x5_E1				Cube_6x6x6_E1			
	K=3	K=4	K=5	K=6	K=3	K=4	K=5	K=6	K=3	K=4	K=5	K=6
[Gontier 2020]	8	5	5	1	9	8	8	1	3	1	8	1
Our Approach	8	6	8	5	11	16	14	13	15	20	27	17

Table 3. Performance of our approach for generating K-piece level-L interlocking $5 \times 5 \times 5$ Cubes with a single hole voxel. The computational time of each result is in minutes.

	K=4	K=6	K=8
L=4	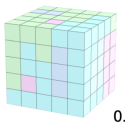 0.028	 0.057	 1.463
L=8	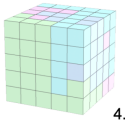 4.540	 3.909	 62.011
L=12	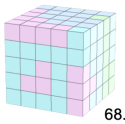 68.272	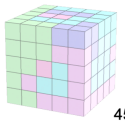 45.643	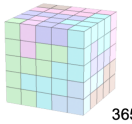 365.675
L=16	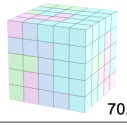 70.757		

Fig. 14. Our fabrication results. From top to bottom, Cube, Sofa, Airplane, Cow, and Owl.

piece can be at any discrete position of the puzzle, and $E = V^2 = N^{2K}$ assuming every pair of vertices is connected by an edge. Hence, the complexity of the design problem is $O(K^N) \cdot O(N^K + N^{2K}) = O(K^N \cdot N^{2K})$. Due to the high complexity of the design problem, our paper focuses on addressing the problem in a small scale, i.e., $K \leq 8$ and $N \leq 1000$.

Despite the high complexity of the problem, our design approach is able to find a solution in the huge design space using a reasonable amount of time. We evaluate the performance of our design approach on a $5 \times 5 \times 5$ Cube with a single hole voxel at the center; see Table 3. The computation time of our approach increases with respect to the number of puzzle pieces K since a larger K means each puzzle piece has fewer number of voxels, making them harder to interlock. The computation time of our approach also increases with respect to the target level of difficulty L since a larger L means that the puzzle has to be interlocking in a larger number of configurations. Our approach is efficient when $K \leq 6$ and $L \leq 8$, e.g., less than 5 minutes for the $5 \times 5 \times 5$ Cubes.

Comparison with [Gontier 2020]. We compare our design approach with a baseline approach [Gontier 2020]. The baseline approach uses a genetic algorithm to generate high-level interlocking puzzles, in which each puzzle candidate (encoded as a 1D array) is an individual and the fitness function is the level of difficulty. To ensure a fair comparison, we re-implemented the baseline approach in C++ and replaced the disassembly planner with ours to compute the exact level of difficulty. We ran both approaches for 12 hours to generate high-level interlocking Cubes with different resolutions, and recorded the puzzle with the highest level of difficulty; see Table 2. When the Cube puzzle has a low resolution (i.e. $4 \times 4 \times 4$) and a small number of pieces (i.e., $K \leq 4$), the two approaches have comparable performance. However, our approach has significantly better performance than the baseline when the puzzle has a higher resolution and/or a larger number of pieces, demonstrating its good scalability to a large design space.

Physical puzzles. We fabricated five of our designed puzzles using a Stratasys J750 multi-color 3D printer; see Figure 14. When playing these puzzles, we found that a larger number (K) of puzzle pieces makes the puzzle harder to play; e.g., the 5-piece Airplane is harder to play than the 4-piece Sofa. This is because one needs more effort to hold the puzzle pieces steadily so they remain in the correct position of each configuration in order to make the next move. We

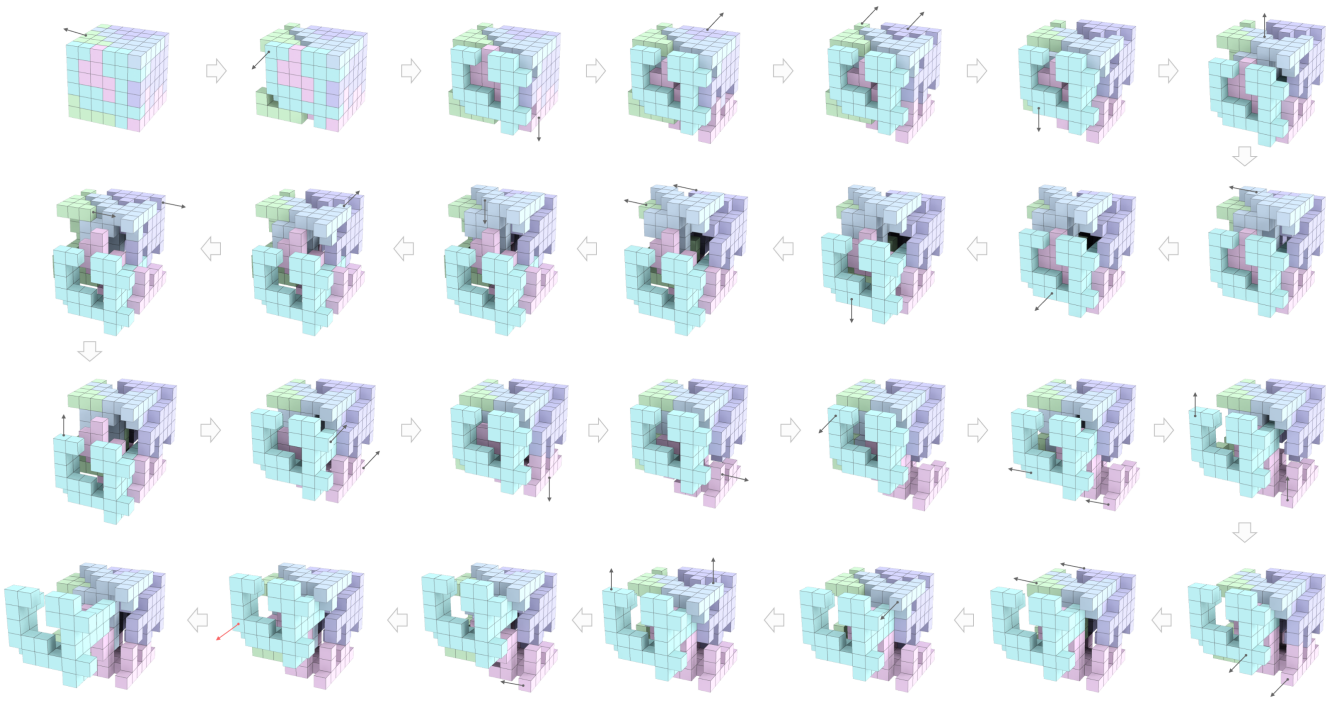

Fig. 15. A kernel disassembly plan to take out the first puzzle piece (in cyan) from a 5-piece level-27 $6 \times 6 \times 6$ Cube designed by our approach.

also found that the time to solve the puzzle increases significantly with the level of difficulty L. We argue that this is because a large L usually means a large kernel disassembly graph, requiring one to explore a large space of puzzle configurations to solve the puzzle.

User study. We conducted a user study to learn how difficult for general users to play our high-level interlocking puzzles. Besides the level-16 Cube, level-8 Sofa, and level-7 Owl shown in Figure 14, we prepared two more puzzles for the user study, a level-4 Cube and a level-8 Cube. We recruited 8 participants, 4 males and 4 females, to play the five 3D printed puzzles, and recorded the time to solve each puzzle for each participant. We found that the average time to solve the puzzles increases with the puzzles' level of difficulty (e.g., 0.30 mins, 0.35 mins, and 7.02 mins for the level-4, -8, and -16 Cubes respectively). In particular, four participants failed to solve the level-16 Cube, due to its very high level of difficulty. One interesting observation is that the time to solve a puzzle depends not only on the level of difficulty but also on the kernel disassembly graph's size. For example, all the participants took a much longer time to solve the level-8 Sofa than the level-8 Cube (i.e., 1.87 mins vs 0.35 mins on average), likely because that the Sofa (307 graph nodes) has a much larger kernel disassembly graph than the Cube (11 graph nodes). After the user study, seven participants chose the Owl as the most attractive puzzle because of its cute appearance. Our user study confirms the necessity of using our computational tool to design interlocking puzzles such that their level of difficulty matches the ability of the user and their appearance can be attractive to the user. Please refer to the supplementary material for more details about our user study.

8 CONCLUSION

This paper presents a computational approach for designing high-level interlocking puzzles from an input voxelized shape. For this purpose, we propose a disassembly planner that is able to compute a given puzzle's exact level of difficulty by enumerating all possible non-monotone, linear/non-linear disassembly plans to take out the first subassembly using a rooted graph data structure. We also present a computational framework that constructs the geometry of each puzzle piece iteratively guided by the disassembly planner, aiming to achieve a user-specified level of difficulty. To extend our approach for designing puzzles with smooth appearance, we formulate and solve a new shape optimization problem for creating voxelizations with a minimal number of problematic voxels. We demonstrate the effectiveness of our approach by designing puzzles with various shapes and topologies, show the advantages of our approach by comparing it with a baseline, and evaluate the difficulty of playing our designed puzzles in a user study.

Limitations and future work. First, our shape optimization focuses on minimizing the number of problematic voxels yet does not consider other requirements such as aesthetics and shape symmetry. Second, our puzzle design approach requires a large internal volume of the input shape for making the puzzle pieces interlocking in multiple configurations. Thus, it may fail for input shapes with no or small internal volume such as architectural shells and tree-like shapes. Third, we found that a high-level interlocking puzzle may be hard to play if the puzzle is not stable in some configurations. One possible way to address this limitation is to incorporate structural stability analysis [Wang et al. 2021] into our computational design

framework. Lastly, our puzzle design approach assumes that the input shape is represented as a voxelization. In the future, we want to extend our approach to support designing high-level interlocking puzzles with other geometric forms such as Japanese Puzzle Boxes with planar parts and integral joints as well as Excalibur Puzzles with a big cube frame that holds the other small puzzle pieces.

ACKNOWLEDGMENTS

We thank the reviewers for the valuable comments, David Gontier for sharing the source code of the baseline design approach, Christian Hafner for proofreading the paper, Keenan Crane for the 3D model of Cow, and Thingiverse for the 3D models of Moai and Owl. This work was supported by the SUTD Start-up Research Grant (Number: SRG ISTD 2019 148), the Swiss National Science Foundation (NCCR Digital Fabrication Agreement #51NF40-141853), and the European Research Council (ERC) under the European Union's Horizon 2020 research and innovation programme (Grant Agreement No 715767 – MATERIALIZABLE).

REFERENCES

Maneesh Agrawala, Doantam Phan, Julie Heiser, John Haymaker, Jeff Klingner, Pat Hanrahan, and Barbara Tversky. 2003. Designing Effective Step-By-Step Assembly Instructions. *ACM Trans. on Graph. (SIGGRAPH)* 22, 3 (2003), 828–837.

Bernd Bickel, Paolo Cignoni, Luigi Malomo, and Nico Pietroni. 2018. State of the Art on Stylized Fabrication. *Comp. Graph. Forum* 37, 6 (2018), 325–342.

A. Bourjault. 1984. *Contribution a une approche méthodologique de l'assemblage automatisé: Elaboration automatique des séquences opératiores.* Ph.D. Dissertation. L'Université de Franche-Comté.

Stewart T. Coffin. 2006. *Geometric Puzzle Design.* A. K. Peters.

Bill Cutler. 1988. Holey 6-Piece Burr! A Collection and Computer Analysis of Unusual Designs. http://billcutlerpuzzles.com/docs/H6PB/index.html .

Ruta Desai, James McCann, and Stelian Coros. 2018. Assembly-aware Design of Printable Electromechanical Devices. In *Proc. ACM UIST*. 457–472.

Mario Deuss, Daniele Panozzo, Emily Whiting, Yang Liu, Philippe Block, Olga Sorkine-Hornung, and Mark Pauly. 2014. Assembling Self-Supporting Structures. *ACM Trans. on Graph. (SIGGRAPH Asia)* 33, 6 (2014), 214:1–214:10.

Noah Duncan, Lap-Fai Yu, Sai-Kit Yeung, and Demetri Terzopoulos. 2017. Approximate Dissections. *ACM Trans. on Graph. (SIGGRAPH Asia)* 36, 6 (2017), 182:1–182:14.

Gershon Elber and Myung-Soo Kim. 2022. Synthesis of 3D Jigsaw Puzzles over Freeform 2-Manifolds. *Comp. & Graph. (SMI)* 102 (2022), 339–348.

Thomas L. De Fazio and Daniel E. Whitney. 1987. Simplified Generation of All Mechanical Assembly Sequences. *IEEE Journal on Robotics and Automation* RA-3, 6 (1987), 640–658.

Chi-Wing Fu, Peng Song, Xiaoqi Yan, Lee Wei Yang, Pradeep Kumar Jayaraman, and Daniel Cohen-Or. 2015. Computational Interlocking Furniture Assembly. *ACM Trans. on Graph. (SIGGRAPH)* 34, 4 (2015), 91:1–91:11.

Somayé Ghandi and Ellips Masehian. 2015. Review and Taxonomies of Assembly and Disassembly Path Planning Problems and Approaches. *Computer-Aided Design* 67-68 (2015), 58–86.

David Gontier. 2020. Multi-level Interlocking Cubes. https://www.ceremade.dauphine.fr/~gontier/Puzzles/InterlockingPuzzles/interlocking.html.

Jianwei Guo, Dong-Ming Yan, Er Li, Weiming Dong, Peter Wonka, and Xiaopeng Zhang. 2013. Illustrating the Disassembly of 3D Models. *Comp. & Graph. (SMI)* 37, 6 (2013), 574–581.

D. Halperin, J.-C. Latombe, , and R. H. Wilson. 2000. A General Framework for Assembly Planning: The Motion Space Approach. *Algorithmica* 26, 3–4 (2000), 577–601.

IBM Research. 1997. The burr puzzles site. https://www.cs.brandeis.edu/~storer/JimPuzzles/BURR/000BURR/READING/IbmPage.pdf.

Alec Jacobson, Daniele Panozzo, et al. 2018. libigl: A simple C++ geometry processing library. https://libigl.github.io/ .

P. Jiménez. 2013. Survey on Assembly Sequencing: A Combinatorial and Geometrical Perspective. *Journal of Intelligent Manufacturing* 24, 2 (2013), 235–250.

Gene T.C. Kao, Axel Körner, Daniel Sonntag, Long Nguyen, Achim Menges, and Jan Knippers. 2017. Assembly-aware Design of Masonry Shell Structures: A Computational Approach. In *Proceedings of the International Association for Shell and Spatial Structures Symposium.*

Lydia Kavraki, Jean-Claude Latombe, and Randall H. Wilson. 1993. On the Complexity of Assembly Partitioning. *Inform. Process. Lett.* 48, 5 (1993), 229–235.

Bernhard Kerbl, Denis Kalkofen, Markus Steinberger, and Dieter Schmalstieg. 2015. Interactive Disassembly Planning for Complex Objects. *Comp. Graph. Forum (Eurographics)* 34, 2 (2015), 287–297.

Naoki Kita and Kazunori Miyata. 2020. Computational Design of Polyomino Puzzles. *The Visual Computer (CGI)* (2020), 1–11.

Naoki Kita and Takafumi Saito. 2020. Computational Design of Generalized Centrifugal Puzzles. *Comp. & Graph. (SMI)* 90 (2020), 21–28.

Duc Thanh Le, Juan Cortés, and Thierry Siméon. 2009. A Path Planning Approach to (Dis)Assembly Sequencing. In *Proc. Int. Conf. on Automation Science and Engineering*. 286–291.

Shuhua Li, Ali Mahdavi-amiri, Ruizhen Hu, Han Liu, Chanqing Zou, Oliver Van Kaick, Xiuping Liu, Hui Huang, and Hao Zhang. 2018. Construction and Fabrication of Reversible Shape Transforms. *ACM Trans. on Graph. (SIGGRAPH Asia)* 37, 6 (2018), 190:1–190:14.

Kui-Yip Lo, Chi-Wing Fu, and Hongwei Li. 2009. 3D Polyomino Puzzle. *ACM Trans. on Graph. (SIGGRAPH Asia)* 28, 5 (2009), 157:1–157:8.

Ellips Masehian and Somayé Ghandi. 2020. ASPPR: A New Assembly Sequence and Path Planner/Replanner for Monotone and Nonmonotone Assembly Planning. *Computer-Aided Design* 123 (2020), 102828:1–102828:22.

Ellips Masehian and Somayé Ghandi. 2021. Assembly Sequence and Path Planning for Monotone and Nonmonotone Assemblies with Rigid and Flexible Parts. *Robotics and Computer-Integrated Manufacturing* 72 (2021), 102180:1–102180:23.

Luiz S. Homem De Mello and Arthur C. Sanderson. 1990. AND/OR Graph Representation of Assembly Plans. *IEEE Transactions on Robotics and Automation* 6, 2 (1990), 188–199.

Fakir S. Nooruddin and Greg Turk. 2003. Simplification and Repair of Polygonal Models Using Volumetric Techniques. *IEEE Trans. Vis. & Comp. Graphics* 9, 2 (2003), 191–205.

Andreas Röver. 2013. Burr Tools. http://burrtools.sourceforge.net/.

Peng Song, Bailin Deng, Ziqi Wang, Zhichao Dong, Wei Li, Chi-Wing Fu, and Ligang Liu. 2016. CofiFab: Coarse-to-Fine Fabrication of Large 3D Objects. *ACM Trans. on Graph. (SIGGRAPH)* 35, 4 (2016), 45:1–45:11.

Peng Song, Chi-Wing Fu, and Daniel Cohen-Or. 2012. Recursive Interlocking Puzzles. *ACM Trans. on Graph. (SIGGRAPH Asia)* 31, 6 (2012), 128:1–128:10.

Peng Song, Chi-Wing Fu, Yueming Jin, Hongfei Xu, Ligang Liu, Pheng-Ann Heng, and Daniel Cohen-Or. 2017. Reconfigurable Interlocking Furniture. *ACM Trans. on Graph. (SIGGRAPH Asia)* 36, 6 (2017), 174:1–174:14.

Peng Song, Zhongqi Fu, Ligang Liu, and Chi-Wing Fu. 2015. Printing 3D Objects with Interlocking Parts. *Comp. Aided Geom. Des. (GMP)* 35-36 (2015), 137–148.

Olga Sorkine and Marc Alexa. 2007. As-Rigid-As-Possible Surface Modeling. In *Proc. Eurographics Symposium on Geometry Processing*. 109–116.

Timothy Sun and Changxi Zheng. 2015. Computational Design of Twisty Joints and Puzzles. *ACM Trans. on Graph. (SIGGRAPH)* 34, 4 (2015), 101:1–101:11.

Keke Tang, Peng Song, Xiaofei Wang, Bailin Deng, Chi-Wing Fu, and Ligang Liu. 2019. Computational Design of Steady 3D Dissection Puzzles. *Comp. Graph. Forum (Eurographics)* 38, 2 (2019), 291–303.

Jungfu Tsao and Jan Wolter. 1993. Assembly Planning with Intermediate States. In *Proc. IEEE Int. Conf. on Robotics and Automation*. 71–76.

Ziqi Wang, Peng Song, Florin Isvoranu, and Mark Pauly. 2019. Design and Structural Optimization of Topological Interlocking Assemblies. *ACM Trans. on Graph. (SIGGRAPH Asia)* 38, 6 (2019), 193:1–193:13.

Ziqi Wang, Peng Song, and Mark Pauly. 2018. DESIA: A General Framework for Designing Interlocking Assemblies. *ACM Trans. on Graph. (SIGGRAPH Asia)* 37, 6 (2018), 191:1–191:14.

Ziqi Wang, Peng Song, and Mark Pauly. 2021. State of the Art on Computational Design of Assemblies with Rigid Parts. *Comp. Graph. Forum (Eurographics)* 40, 2 (2021), 633–657.

Jan D. Wolter. 1991. A Combinatorial Analysis of Enumerative Data Structures for Assembly Planning. In *Proc. IEEE Int. Conf. on Robotics and Automation*. 611–618.

Chenming Wu, Haisen Zhao, Chandrakana Nandi, Jeffrey I. Lipton, Zachary Tatlock, and Adriana Schulz. 2019. Carpentry Compiler. *ACM Trans. on Graph. (SIGGRAPH Asia)* 38, 6 (2019), 195:1–195:14.

Shi-Qing Xin, Chi-Fu Lai, Chi-Wing Fu, Tien-Tsin Wong, Ying He, and Daniel Cohen-Or. 2011. Making Burr Puzzles from 3D Models. *ACM Trans. on Graph. (SIGGRAPH)* 30, 4 (2011), 97:1–97:8.

Miaojun Yao, Zhili Chen, Weiwei Xu, and Huamin Wang. 2017. Modeling, Evaluation and Optimization of Interlocking Shell Pieces. *Comp. Graph. Forum (Pacific Graphics)* 36, 7 (2017), 1–13.

Yinan Zhang and Devin Balkcom. 2016. Interlocking Structure Assembly with Voxels. In *Proc. IEEE/RSJ Intl. Conf. on Intelligent Robots and Systems*. 2173–2180.

Yinan Zhang, Yotto Koga, and Devin Balkcom. 2021. Interlocking Block Assembly With Robots. *IEEE Transactions on Automation Science and Engineering* 18, 3 (2021), 902–916.

Yahan Zhou and Rui Wang. 2012. An Algorithm for Creating Geometric Dissection Puzzles. In *Proc. Bridges Towson: Mathematics, Music, Art, Architecture, Culture*. 49–56.